Journal of Power Sources 265 (2014) 273–281

Contents lists available at ScienceDirect

Journal of Power Sources

journal homepage: www.elsevier.com/locate/jpowsour

A facile electrochemical fabrication of hierarchically structured nickel–copper composite electrodes on nickel foam for hydrogen evolution reaction

Zuwei Yin, Fuyi Chen*

State Key Laboratory of Solidification Processing, Northwestern Polytechnical University, Xian 710072, China

HIGHLIGHTS

- We prepare 3D NiCu precursor by galvanic replacement reaction between Ni foam and copper ion.
- $CuCl_2$ is the best dipping solution because the formation and hydrolysis of $CuCl_n^{1-n}$.
- An activation process was done to remove the oxide.
- CV treatment was done to fabricate a hierarchical architectural structure.
- The hierarchical architectural NiCu electrode has the best HER activity of all the electrodes.

ARTICLE INFO

Article history:
Received 22 January 2014
Received in revised form
12 April 2014
Accepted 27 April 2014
Available online 9 May 2014

Keywords:
Hydrogen evolution reaction (HER)
Galvanic replacement reaction (GRR)
Cyclic voltammetry (CV) treatment
Hierarchical structure
Nickel–copper electrodes

ABSTRACT

A NiCu composite electrode with hierarchical structure has been successfully fabricated by an electrochemical method, which consisted of galvanic replacement reaction (GRR), activation process and cyclic voltammetry (CV) treatment. The three-dimensional (3D) Ni–Cu precursors were prepared firstly by dipping Ni foam into three kinds of different copper ion solutions and identified that $CuCl_2$ is a favorite electrolyte. This may be attributed to the adsorption of chloride ion on copper surface to form the $CuCl_n^{1-n}$ complex and the hydrolysis of $CuCl_n^{1-n}$. After an activation process to reduce the hydrolytic product Cu_2O into Cu, a CV treatment was performed to form a hierarchical structure to improve the surface area and to heighten the hydrogen evolution reaction (HER) activity. The optimal number of CV cycles is 3.

1. Introduction

Growing concerns about global warming and energy security have necessitated the realization of renewable sources as a viable alternative to fossil-fuel-based technologies. Because hydrogen is the cleanest energy source and an ideal energy carrier, several researchers have focused on its production methods. Among the various approaches designed to produce hydrogen, alkaline water electrolysis HSN proven to be a promising method [1–3]. Its advantages over other hydrogen production methods include the use of water as a feedstock as its availability is relatively unlimited and can be procured from almost any part of the planet. Moreover, high-purity hydrogen in large quantities can be obtained in this manner [4]. However, the primary problems in the production of electrolytic hydrogen are the high costs involved and high energy consumption. To make this technique more efficient and economical, it is imperative to select inexpensive electrode materials that exhibit good hydrogen evolution reaction (HER) activity.

The ideal properties of an electrode used for water electrolysis are (i) large surface area, (ii) good electrical conductivity, (iii) good stability, (iv) low over-potential, (v) low cost and (vi) ease of fabrication [5]. Due to its high HER activity, good corrosion resistance, abundant availability and relatively low cost, nickel and its alloys are some of the most studied non-precious electrode materials for alkaline water electrolysis [6–8].

Galvanic replacement reaction (GRR) is a type of single-step reaction that utilizes the differences between the standard electrode potentials of various elements, resulting in the deposition of nobler elements and the dissolution of lesser noble components [9]. Usually, it only requires a beaker and consumes almost zero

* Corresponding author. Tel./fax: +86 29 88492052.
E-mail address: fuyichen@nwpu.edu.cn (F. Chen).

http://dx.doi.org/10.1016/j.jpowsour.2014.04.123
0378-7753/

energy. The electroless nature of GRR affords them the unique and significant advantage of simplicity. Recently, it was employed to fabricate several electrocatalysts for various reactions. However, noble metals have been primarily investigated, such as Pt, Pd, Au, and Ag [10–13]. Only a few studies involving catalysts prepared for the HER have been undertaken. In our study, we prepared the NiCu precursor for hydrogen evolution by means of GRR between Ni foam and Cu^{2+}.

Cyclic voltammetry (CV) treatment has been used to roughen the porous electrodes and produce hydroxide for the electrochemical capacitors [14]. In our previous paper [15], we performed deposition–dealloying cycling before selective electrochemical dissolution to fabricate a hierarchical porous structure. In the present study, we conducted a deposition–dealloying cycling treatment after GRR to obtain hierarchically structured NiCu (HSN) electrodes with better HER activity.

Among the Ni-based electrodes under investigation, NiCu has shown potential for using as a cathode during alkaline HER. Initially, Solmaz et al. [16] reported that electrodeposited NiCu alloy could prove to be an efficient HER catalyst in a KOH solution. The stability and corrosion behavior with long-term electrolysis was also investigated [17]. Wang et al. [18] obtained a porous 3D NiCuCo nano-network structure by means of a facile electrodeposition method; the electrodeposition parameter was also discussed. Giz et al. [19] obtained a NiCuFe alloy in an acetate bath by electrochemical co-deposition, which exhibited good stability in a chlor-alkaline solution. They adopted the conventional electrodeposition technique to fabricate NiCu-based alloys. This process consumed a large amount of time; therefore, we replaced it with a rapid brush plating method as compared to that in our earlier study. Both these methods need relatively complex equipment and consume large amounts of energy.

In this study, we fabricated a 3D NiCu precursor by dipping Ni foam in a copper ion solution, which requires simpler equipment and consumes lower energy than conventional electrodeposition techniques and brush plating methods. The effect of the anion was also discussed; $CuCl_2$ solution was selected as the dipping solution. Then, an activation process was employed and a HSN electrode was prepared using the CV treatment. The electrocatalytic performance of the developed electrodes in terms of HER was evaluated using a 1 M KOH solution based on their cathodic polarization curves and electrochemical impedance spectroscopy (EIS) data. The results confirmed that a combination of GRR and CV treatment can yield high HER activity of NiCu composite electrodes.

2. Experimental

2.1. Electrode fabrication

2.1.1. Fabrication of NiCu precursors

The NiCu precursors were obtained by immersing Ni foam in a copper ion solution. Before performing GRR, the Ni foam was degreased with acetone and dipped in 0.1 M H_2SO_4 solution for 15 min to remove the oxide on the surface. All the instances of the Ni foam had an exposure surface area of 1 cm^2 to the solution. The other surface was covered with resin.

The copper ion concentration was maintained at 0.5 M, and $CuCl_2$, $CuSO_4$ and $Cu(NO_3)_2$ solutions were selected. Different instances of Ni foam were dipped in these three solutions. For each dipping solution, the immersing time was set as 0.5 h, 1 h, 1.5 h, 2 h, 3 h and 4 h. The HER activity for all the electrodes was measured, and the dipping solution with the optimum dipping time was selected.

2.1.2. Activation process

The results confirmed that the $CuCl_2$ solution was the most suitable for fabricating NiCu precursors by using GRR. Further, electrode dipping in 0.5 M $CuCl_2$ for 1 h exhibited the highest HER activity. Therefore, we selected this electrode to fabricate HSN electrodes. Here, we need to remove the hydrolytic product Cu_2O from the Ni foam dipped in $CuCl_2$ solution.

A conventional three-electrode cell system was formulated, and the selected NiCu precursor was used as the working electrode. The saturated calomel electrode (SCE) was used as the reference electrode and gauze platinum electrode, the auxiliary electrode. Constant-potential electrolysis was performed at −1.6 V for 20 min in order to reduce Cu_2O to Cu. The current–time curves were recorded.

2.1.3. CV treatment

After the activation process, CV treatment was performed. A typical three-electrode cell system was formulated and the prepared NiCu was used as the working electrode. The solution comprised a mixture of 0.02 M $CuSO_4$, 0.3 M $NiSO_4$ and 0.2 M $Na_3C_6H_5O_7$ at a pH of 4. The pH was adjusted by means of H_2SO_4 solution. CV treatment was performed between −1.0 V and 0.4 V versus SCE at a scan rate of 10 mV s^{-1} for 1, 2, 3, 4 and 5 cycles. By means of deposition–dealloying cycling, we can get HSN electrodes because of the 3D NiCu precursors. The obtained electrodes were labeled as HSN-1, HSN-2, HSN-3, HSN-4 and HSN-5.

2.2. Physical characterization

The morphologies and chemical compositions of the samples were examined using a scanning electron microscope (SEM; Tescan Vega 3) and an auxiliary X-ray energy dispersive spectroscope (EDS), respectively. The measurements were conducted at an acceleration potential of 20 keV. X-ray diffraction (XRD) was performed using an X'Pert PRO X-ray diffractometer (PANalytical) to investigate the crystal structures. The diffractograms were measured at room temperature between 10° and 90° (2θ) under a goniometer speed of 2°/min.

2.3. Electrochemical measurements

The electrochemical measurements were carried out using the CHI660C electrochemical workstation (Chenhua Instrument Company). A typical three-electrode setup was used. The fabricated electrodes served as the working electrode; SCE, the reference electrode; and Au electrode, the auxiliary electrode. All the tests were performed in 1 M KOH solution at room temperature. Before tests, the KOH solution was purified by nitrogen for 30 min. The Purpose is to remove oxygen and carbon dioxide. Then we made a constant-potential electrolysis at −1.6 V to remove the inpurities brought by electrode itself. All the working electrodes had an exposure surface area of 1 cm^2 to the solution. The other surface was covered with resin. The cathodic polarization curves were obtained, and the EIS experiments were conducted. The scan rate for polarization measurements was maintained at 1 mV s^{-1}. The EIS measurements were performed at an input signal amplitude of 5 mV, and the measurement frequency range was set from 100 kHz to 10 mHz. The measured data were fitted by means of the Zview software.

3. Results and discussion

3.1. Preparation of 3D NiCu precursors

3.1.1. Selection of dipping solution

Here, 3D NiCu precursors were fabricated by means of GRR between Ni foam and Cu^{2+}, and the dipping solution with the

optimum dipping time was selected. We selected $CuSO_4$, $Cu(NO_3)_2$ and $CuCl_2$ as the dipping solutions. Different instances of Ni foam were dipped in each solution for 0.5 h, 1 h, 1.5 h, 2 h, 3 h and 4 h.

Fig. 1 shows the polarization curves of Ni foam and 3D NiCu electrodes obtained by immersing Ni foam in 0.5 M $CuSO_4$ solution for different times. The tests were undertaken in a 1 M KOH solution. The SCE was used as the reference electrode, so the reversible potential for hydrogen evolution was approximately −1.07 V. The HER over-potential region exists from −1.1 V to −1.4 V. Evidently, dipping Ni foam in $CuSO_4$ solution improved the HER activity of Ni foam in a precise manner. In the main HER over-potential region, Ni foam exhibits the lowest HER activity; it was the maximum for a dipping time of 2 h. When the dipping time is less than 2 h, the HER activity of the fabricated 3D NiCu increases with time. However, it decreases with increasing time when the dipping time is larger than 2 h.

Fig. 2 displays the polarization curves of Ni foam and 3D NiCu electrodes in a 1 M KOH solution; the electrodes were obtained by immersing Ni foam in 0.5 M $Cu(NO_3)_2$ solution for different times. Evidently, Ni foam exhibits the lowest HER activity, and the NiCu electrode obtained by immersing Ni foam in 0.5 M $Cu(NO_3)_2$ for 2 h exhibits the highest HER activity.

Fig. 3 shows the polarization curves of Ni foam and 3D NiCu electrodes obtained by immersing Ni foam in 0.5 M $CuCl_2$ solution for different times. In the main HER region between −1.2 V and −1.4 V, Ni foam exhibits the lowest HER activity; the highest HER activity exists when the dipping time is 1 h. In the region between −1.1 V and −1.2 V, the NiCu electrode fabricated by immersing Ni foam in 0.5 M $Cu(NO_3)_2$ for 2 h exhibits a higher HER activity, but the difference is marginal.

From the above, it is clear that dipping Ni foam in 0.5 M $CuSO_4$, $Cu(NO_3)_2$ and $CuCl_2$ solutions is optimum for times of 2 h, 2 h and 1 h, respectively. Fig. 4a shows the polarization curves of Ni foam and 3D NiCu electrodes obtained by immersing Ni foam in 0.5 M $CuSO_4$ for 2 h, 0.5 M $Cu(NO_3)_2$ for 2 h and 0.5 M $CuCl_2$ for 1 h. It is evident that Ni foam exhibits the lowest HER activity. In the high over-potential region between −1.225 V and −1.4 V, the HER activity of NiCu electrode dipped in 0.5 M $CuCl_2$ for 1 h is the highest and its value is lower than the electrode dipped in 0.5 M $Cu(NO_3)_2$ for 2 h from −1.1 V to −1.225 V. The difference between the two is apparent: additional data is required to determine the electrode that yields the better HER activity.

Fig. 5a–d shows the SEM images of Ni foam and 3D NiCu electrodes obtained by immersing Ni foam in 0.5 M $CuSO_4$ for 2 h, 0.5 M $Cu(NO_3)_2$ for 2 h and 0.5 M $CuCl_2$ for 1 h. The lowest HER activity of

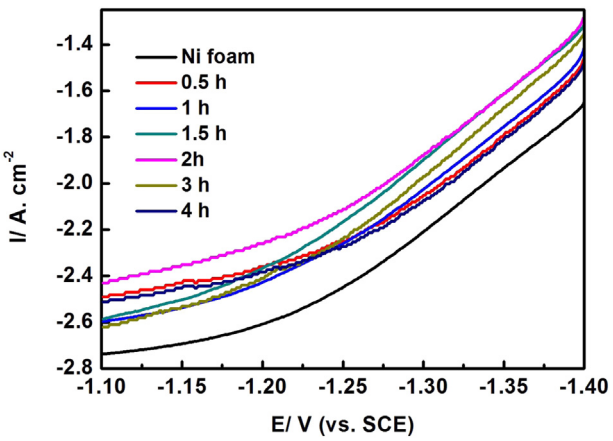

Fig. 1. Polarization curves of Ni foam and 3D NiCu electrodes obtained by immersing Ni foam in 0.5 M $CuSO_4$ solution for different time.

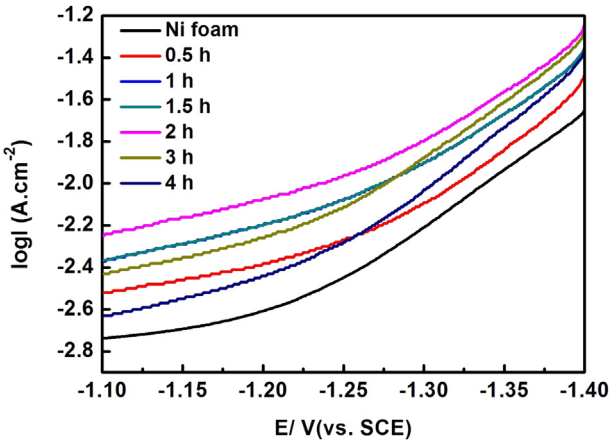

Fig. 2. Polarization curves of Ni foam and 3D NiCu electrodes obtained by immersing Ni foam in 0.5 M $Cu(NO_3)_2$ solution for different time.

Ni foam can be attributed to its smooth surface. The surface of NiCu electrode obtained by immersing Ni foam in 0.5 M $CuCl_2$ for 1 h is the roughest. Moreover, the dipping time required for 0.5 M $CuCl_2$ is lesser. Although the initial current response of the obtained NiCu electrode by dipping Ni foam in 0.5 M $CuCl_2$ for 1 h is not optimal, we believe that this is the best choice for fabricating 3D NiCu precursors.

3.1.2. *Mechanism of 3D NiCu fabrication in $CuCl_2$ solution*

In order to understand the reason for which dipping in $CuCl_2$ solution yields a rougher surface in a shorter time, we provide the SEM images of 3D NiCu electrodes in Fig. 6. These electrodes were obtained by immersing Ni foam in 0.5 M $CuCl_2$ solution for 0.5 h, 1 h, 1.5 h, 2 h, 3 h and 4 h.

First, we know that GRR occurs between Ni and Cu^{2+} when Ni foam is dipped in a copper ion solution [20]:

$$Ni(s) + Cu^{2+}(aq) \rightarrow Ni^{2+}(aq) + Cu(s) \quad (1)$$

According to Droog [21] and Marchiano [22], we know that certain special reactions occur when Cu atom exists in a solution that comprises a chloride ion:

$$Cu + Cl^- \rightarrow \left(CuCl^-\right)_{ad} \quad (2)$$

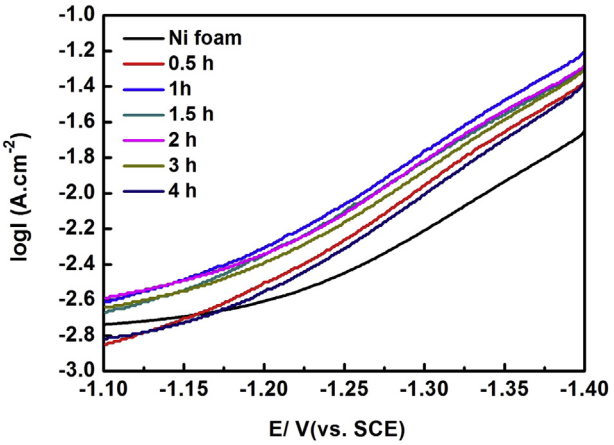

Fig. 3. Polarization curves of Ni foam and 3D NiCu electrodes obtained by immersing Ni foam in 0.5 M $CuCl_2$ solution for different time.

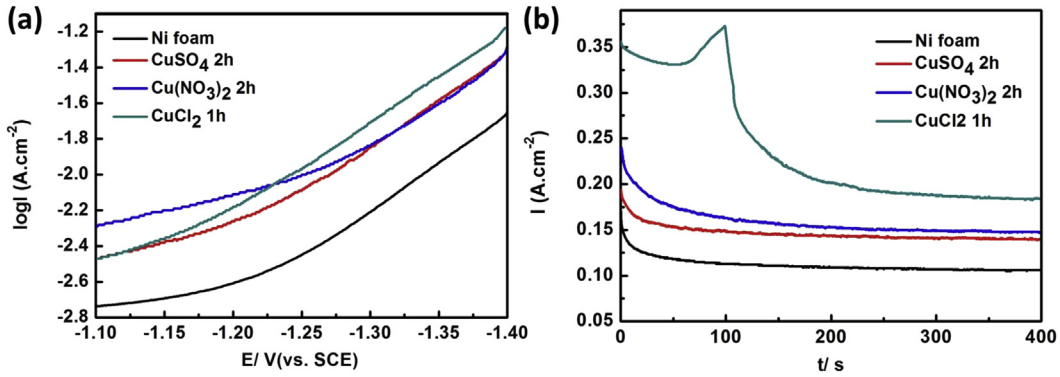

Fig. 4. (a) Polarization curves of Ni foam and 3D NiCu electrodes obtained by immersing Ni foam in 0.5 M $CuSO_4$ for 2 h, 0.5 M $Cu(NO_3)_2$ for 2 h and 0.5 M $CuCl_2$ for 1 h, respectively. (b) Current–time curves of Ni foam and 3D NiCu electrodes obtained by immersing Ni foam in 0.5 M $CuSO_4$ for 2 h, 0.5 M $Cu(NO_3)_2$ for 2 h and 0.5 M $CuCl_2$ for 1 h, respectively.

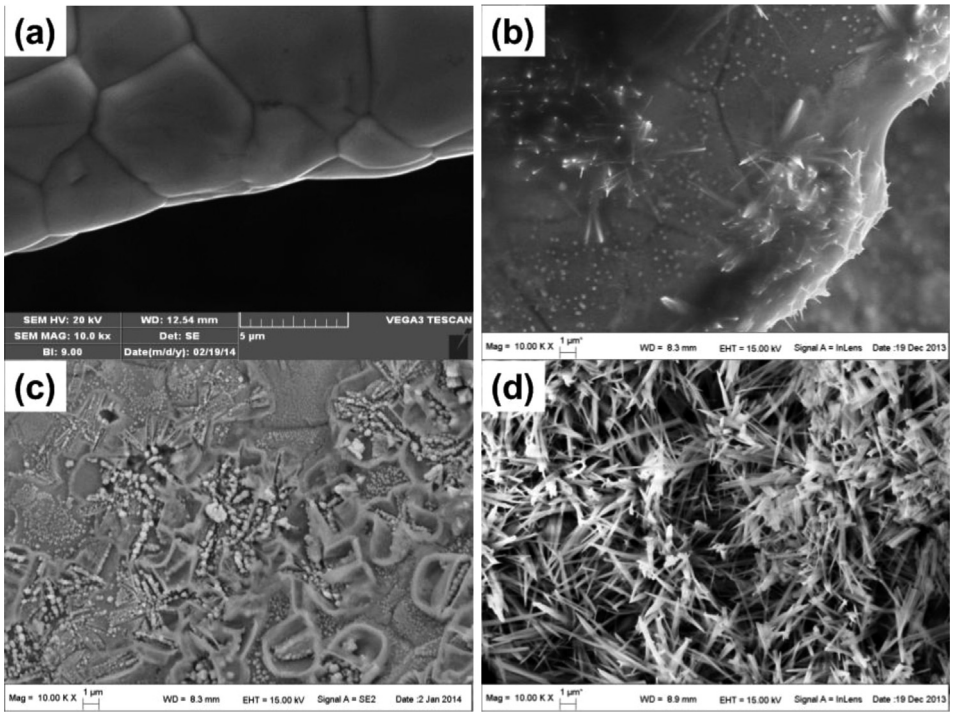

Fig. 5. SEM images of (a) Ni foam and 3D NiCu electrodes obtained by immersing Ni foam in (b) 0.5 M $CuSO_4$ for 2 h, (c) 0.5 M $Cu(NO_3)_2$ for 2 h and (d) 0.5 M $CuCl_2$ for 1 h, respectively.

$$(CuCl^-)_{ad} + (n-1)Cl^- - e \rightarrow Cu_n^{1-n} \quad (3)$$

$$Cu_n^{1-n} + 2OH^- \rightarrow Cu(OH)_2^- + nCl^- \quad (4)$$

$$\text{Then,} \quad 2Cu(OH)_2^- \rightarrow Cu_2O + H_2O + 2OH^- \quad (5)$$

$$\text{Or} \quad 2Cu(OH)_2^- + 2H^+ \rightarrow Cu_2O + 3H_2O \quad (6)$$

Along with GRR, chloride ion gets adsorbed on the copper surface yielding $(CuCl^-)_{ad}$. Thereafter, $CuCl_n^{1-n}$ complex is formed and Cu_2O is formed through the hydrolysis of $CuCl_n^{1-n}$, which promotes GRR between Ni and Cu^{2+}. Therefore, we can get a rougher surface in a shorter time by dipping Ni foam in a $CuCl_2$ solution.

A few Cu_2O octahedrons are distinctly clear in Fig. 6a, which is similar to that obtained by Radi [23]. When the dipping time is 1 h, 1.5 h and 2 h, the Cu_2O octahedron cannot be seen. However, Cu_2O octahedrons are obvious in Fig. 6e, and the size of Cu_2O octahedrons become larger in Fig. 6f. EDS is performed to confirm this speculation, thereby proving that the chemical composition of these octahedrons was Cu_2O.

3.2. Activation process

From the above, we know that $CuCl_2$ is the best dipping solution with an optimum dipping time of 1 h. We have used 3D NiCu electrodes for fabricating HSN electrodes. On the basis of the fabricated 3D NiCu precursors, an activation process was performed. A constant-potential electrolysis was undertaken at −1.6 V for 20 min in a 1 M KOH solution. This was done to remove the oxide on the NiCu surface and to prepare it for the subsequent CV treatment [17].

Fig. 4b shows the current–time curves of Ni foam and 3D NiCu electrodes obtained by immersing Ni foam in 0.5 M $CuSO_4$ for 2 h, 0.5 M $Cu(NO_3)_2$ for 2 h and 0.5 M $CuCl_2$ for 1 h, which were

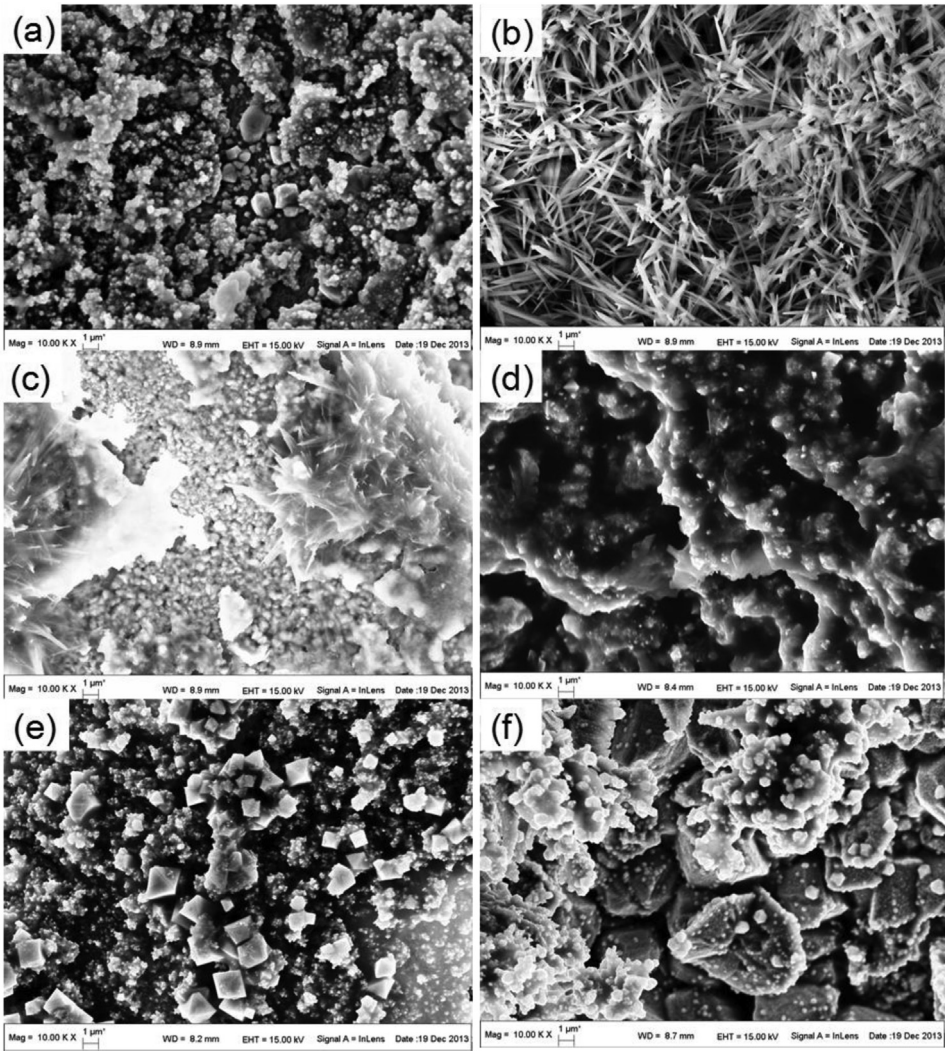

Fig. 6. SEM images of 3D NiCu electrodes obtained by immersing Ni foam in 0.5 M $CuCl_2$ solution for (a) 0.5 h, (b) 1 h, (c) 1.5 h, (d) 2 h, (e) 3 h and (f) 4 h.

measured at −1.6 V. An activation process is evident in the curve of 3D NiCu electrode obtained by immersing Ni foam in 0.5 M $CuCl_2$ for 1 h. In the other curves, this activation process is not observed. This result confirms our previous speculation of the existence of oxide.

Fig. 7a shows the XRD patterns of Ni foam, 3D NiCu electrodes obtained by immersing Ni foam in 0.5 M $CuCl_2$ for 1 h without activation and that obtained with activation. It can be seen that there were Cu_2O (110) and (111) peaks existing after dipping in a $CuCl_2$ solution for 1 h. They subsequently disappeared in the

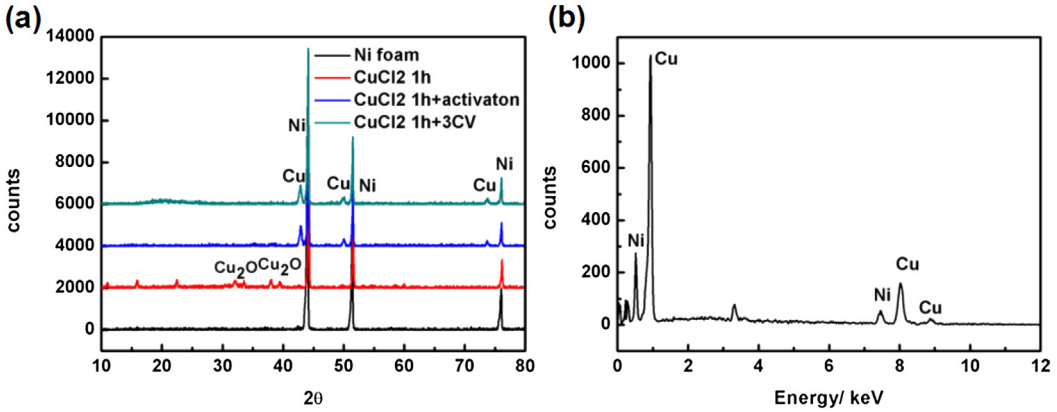

Fig. 7. (a) XRD patterns of Ni foam, 3D NiCu electrodes obtained by immersing Ni foam in 0.5 M $CuCl_2$ solution for 1 h without activation, 3D NiCu electrodes obtained by immersing Ni foam in 0.5 M $CuCl_2$ solution for 1 h with activation and hierarchically structured NiCu electrode experienced 3 deposition–dealloying cycles; (b) EDS spectrum of 3D NiCu electrodes obtained by immersing Ni foam in 0.5 M $CuCl_2$ solution for 1 h with activation.

Table 1
The chemical composition of 3D NiCu electrodes obtained by immersing Ni foam in 0.5 M $CuCl_2$ for different time and keeping −1.6 V in 1 M KOH solution for 20 min.

Element	Immersing time					
	0.5 h	1 h	1.5 h	2 h	3 h	4 h
Ni (at%)	33.18	20.29	17.52	13.12	7.19	0
Cu (at%)	66.82	79.71	82.48	86.88	92.81	100

activated sample and some patterns of Cu are revealed. Further, the results prove the existence of a Cu_2O product in GRR between Ni and $CuCl_2$ solution.

To measure the chemical composition of NiCu precursors obtained by dipping Ni foam in 0.5 M $CuCl_2$ solution for different times, all these electrodes were activated under the same condition. After activation, EDS measurements were performed. The chemical compositions of these NiCu precursors are listed in Table 1. The EDS spectrum of NiCu obtained by immersing in 0.5 M $CuCl_2$ for 1 h is shown in Fig. 7b as an example.

According to Ngamlerdpokin [24], the optimum Ni content in NiCu electrodes is approximately 13 at%. The Ni content in the sample dipped for 2 h is 13.12 at%. As shown in Figs. 3 and 6d, the surface of the 2 h sample is not the roughest, but it exhibits the highest HER activity in the region between −1.1 V and −1.2 V. This can be attributed to its chemical composition.

3.3. Fabrication of HSN electrodes

After the activation process, we conducted a CV treatment to fabricate HSN electrodes. Fig. 7a shows the XRD pattern of HSN-3. As compared to the 3D NiCu electrode fabricated by dipping Ni foam in 0.5 M $CuCl_2$ for 1 h with subsequent activation, all the patterns still exist but with different strengths. This suggests that the CV treatment does not change the surface phase in the electrodes.

Fig. 8 displays the SEM images of NiCu electrodes formed by immersing Ni foam in 0.5 M $CuCl_2$ for 1 h and that of HSN-3. As shown in Fig. 8a, the NiCu precursor has a 3D structure, which leads to the high HER activity. Fig. 8b shows the hierarchical structure of HSN-3. All the other HSN electrodes reveal a similar structure. On the surface of a tree-like structure, a flower-like structure can be seen. This hierarchical structure can yield a higher surface area and improve the HER activity.

The formation of such a hierarchical structure can be attributed to the deposition–dealloying cycling process. In the cathodic deposition process, NiCu was deposited in the gap existing between the NiCu precursors. Further, in the anodic dealloying process, the selective dissolution of Cu occurs in both the NiCu precursor and deposited NiCu, thereby revealing a hierarchical structure.

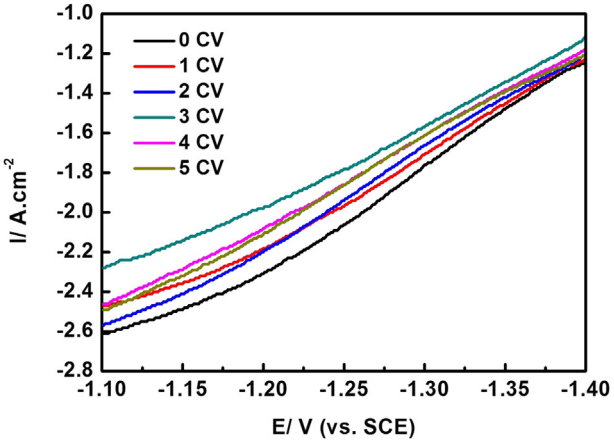

Fig. 9. Polarization curves of hierarchically structured NiCu electrodes experienced immersing in 0.5 M $CuCl_2$ solution for 1 h and CV treatment for different number.

Fig. 9 shows the polarization curves of NiCu electrodes fabricated by immersing Ni foam in 0.5 M $CuCl_2$ solution for 1 h, and subsequently, CV treatment is undertaken for different numbers of cycles. It is obvious that the sample without CV treatment exhibits the lowest HER activity and the sample with 3 CV cycles exhibits the highest HER activity. In the primary hydrogen evolution region, the HER activity of HSN electrode increases with the number of cycles for number of cycles lower than 3. When the number of cycles is higher than 3, the HER activity of the HSN electrode decreases with the number of cycles.

The chemical composition of HSN electrodes for different number of CV cycles is listed in Table 2. It is evident that the Cu content initially increases and then decreases. The optimal Ni/Cu

Table 2
The chemical composition of hierarchical architectural NiCu electrodes experienced different number.

Element	CV number					
	0	1	2	3	4	5
Ni (at%)	20.29	4.73	10.65	16.11	25.77	38.92
Cu (at%)	79.71	95.27	89.35	83.89	74.23	71.08

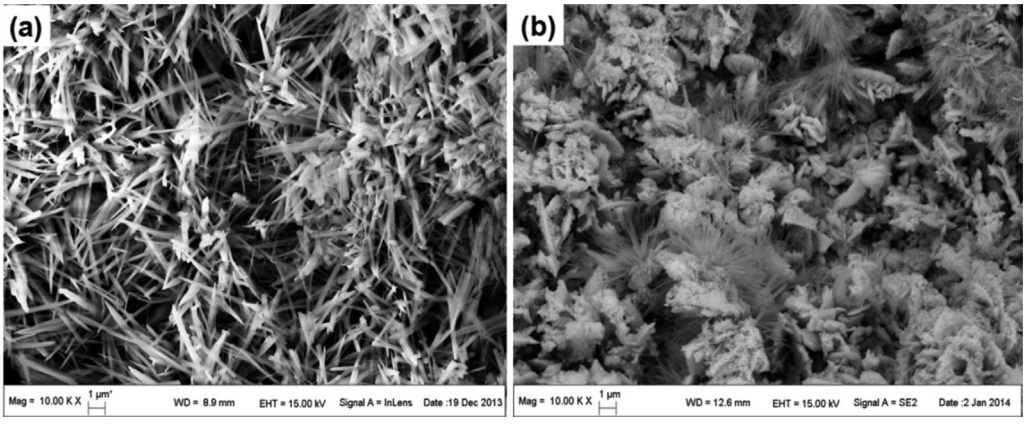

Fig. 8. SEM images of (a) 3D NiCu electrode obtained by immersing Ni foam in 0.5 M $CuCl_2$ for 1 h and (b) hierarchically structured NiCu electrode experienced immersing in 0.5 M $CuCl_2$ for 1 h and 3 CV treatment number (HSN-3).

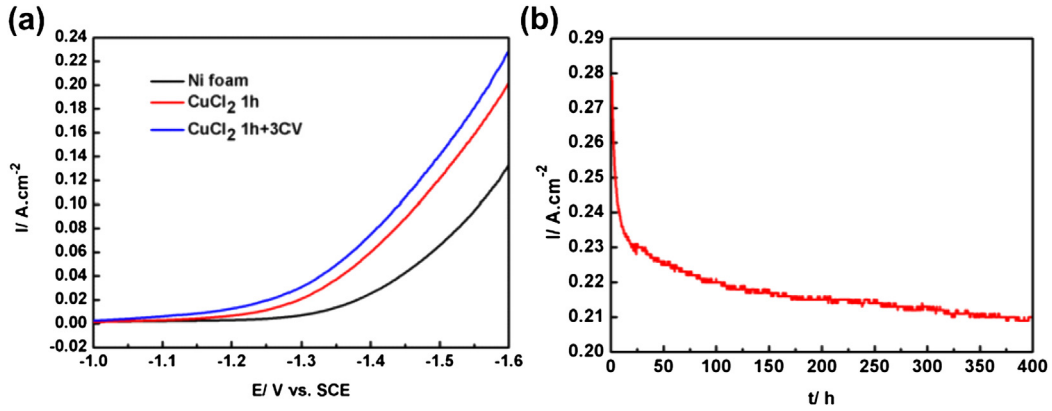

Fig. 10. (a) Current–Potential curves of Ni foam, 3D NiCu electrode obtained by immersing Ni foam in 0.5 M $CuCl_2$ for 1 h and hierarchically structured NiCu electrode experienced immersing in 0.5 M $CuCl_2$ for 1 h and 3 CV treatment number (HSN-3). (b) Current–time curve at −1.6 V of HSN-3.

Table 3
The electrochemical data determined from polarization curves and Nyquist plots at different overpotentials (η).

Working electrodes	$-\eta$ (V)	Polarization curves (mA cm^{-2})	Tafel slop (b/mV dec^{-1})	HER current (i_0/mA cm^{-2})	Electrochemical impedance spectroscopy				
					Rs (Ω)	Rct (Ω)	CPE (F)	n	R_f
Ni foam	0.100	2.37	196.77	0.61274	1.205	74.5	0.0014316	0.81203	71.53
	0.200	4.27	(±2.43)	(±0.04)	1.236	12.36	0.00098594	0.81832	49.317
	0.300	16.3			1.213	2.611	0.00061583	0.85908	30.8165
$CuCl_2$ 1 h	0.100	3.81	198.40	1.47313	1.211	35.6	0.028052	0.84468	1372.6
	0.200	10.87	(±1.65)	(±0.08)	1.097	5.78	0.023768	0.81921	1193.75
	0.300	40.78			1.076	1.432	0.015887	0.81646	797.1
$CuCl_2$ 1 h + 3CV	0.100	8.26	228.31	2.69392	0.991	15.44	0.040113	0.79922	2004.65
	0.200	19.32	(±0.85)	(±0.06)	0.988	4.23	0.033421	0.81513	1670.7
	0.300	56.65			0.972	1.246	0.021365	0.7753	1069.25

ratio exists around 3 CV cycles. This may be one of the factors contributing towards the highest HER activity.

Fig. 10b shows the long-tern current–time curve at −1.6 V of HSN-3. In the origin period of constant-potential electrolysis, a high current can be observed. This can be contributed to the activation process. Then the current decreases slowly, but it is relatively constant. When the time is 100 h, the current is about 220 mA cm^{-2}. When the time is 400 h, the current is about 210 mA cm^{-2}. Our electrode exhibits a good electrochemical stability.

3.4. Comparison

In order to effectively understand our experimental design, we compare Ni foam, NiCu electrode formed by dipping Ni foam in 0.5 M $CuCl_2$ for 1 h and HSN-3. Fig. 10 shows the corresponding polarization curves. A constant-potential electrolysis was undertaken at −1.6 V for 20 min to obtain repeatable data [17]. In order to effectively compare the catalytic activity, the cathodic current densities—directly proportional to the rate of hydrogen evolution—were determined from the corresponding polarization curves for different over-potentials; these values are listed in Table 3.

From Fig. 10 and Table 3, it is evident that the HER activity of Ni foam is the lowest. The low HER activity of Ni foam can be attributed to its smooth surface. Further, the improvement in the HER activity of NiCu, which is formed by dipping Ni foam in 0.5 M $CuCl_2$ for 1 h, can be mainly attributed to its 3D structure. This 3D structure yields a higher surface area. The HER activity of HSN-3 is further improved. HSN-3 has a high current density of 56.65 mA cm^{-2} for an over-potential of −0.300 V, which is slightly higher than 55.80 mA cm^{-2} as reported by Solmaz. The improvement in the HER activity can be attributed to the increase in the actual surface area, indicating that the combination of GRR and CV treatment can be used to fabricate a hierarchical structure.

The EIS measurements were performed for different over-potentials, and the representative Nyquist plots for Ni foam, 3D NiCu electrode obtained by immersing Ni foam in 0.5 M $CuCl_2$ for 1 h and HSN-3 electrodes for an over-potential of −0.200 V are shown in Fig. 11. The EIS data were fitted according to the model of the simple Randle's cell (inset in Fig. 11), and the calculated data are listed in Table 3. As seen from Fig. 11, a slightly depressed capacitive semicircular shape with different radii can be observed for all the samples. The deviation from an ideal semicircle can be attributed to the surface inhomogeneities on the electrodes. The existence of a single loop in the Nyquist plots indicates that the HER is mainly controlled by the charge transfer process. From Fig. 11 and Table 3, it is evident that the HSN-3 electrode has the minimum charge transfer resistance (Rct) and the Ni foam has the maximum value for the same over-potential. The CPE (constant phase element)—representing the surface area of the electrodes [25]—is the maximum in the case of HSN-3 and minimum in the case of Ni foam. The R_f of electrodes in different over-potential, which can be determined by comparison CPE with 20 μF/cm^2, was listed in Table 3. At −0.200 V over-potential, Ni foam has the smallest R_f of 49.317 and HSN-3 has the largest R_f of 1670.7, 3D NiCu electrode obtained by immersing Ni foam in 0.5 M $CuCl_2$ for 1 h has the middle of 1193.75. These data confirmed that GRR and CV treatment can improve the surface area of our electrodes. The parameter n—generally accepted to be a measure of surface inhomogeneity—was lower than 1.0, which suggested that the electrodes have a rough structure (as substantiated by the SEM micrographs). Rs, which represents the solution resistance, is almost the same for the

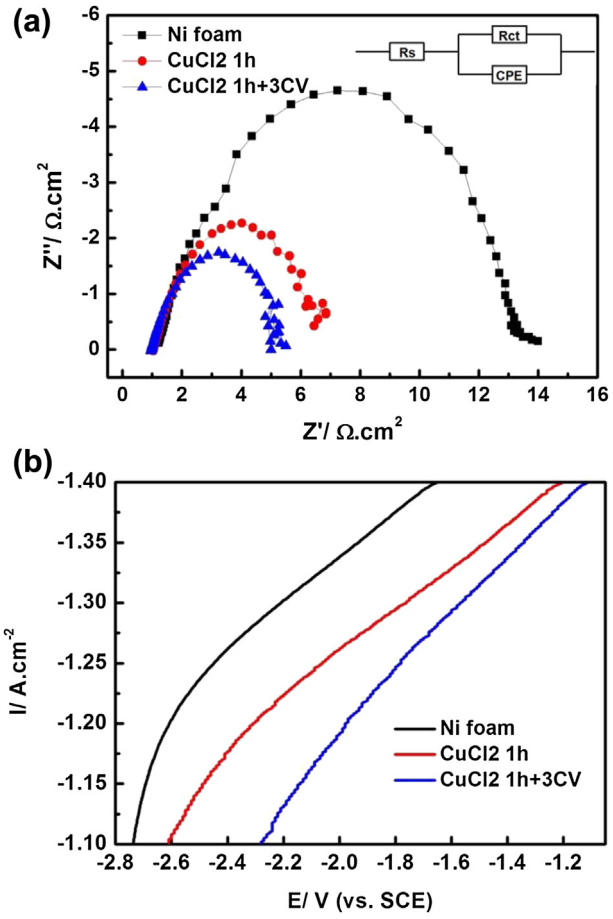

Fig. 11. (a) Nyquist plots of Ni foam, 3D NiCu electrode obtained by immersing Ni foam in 0.5 M $CuCl_2$ for 1 h and hierarchically structured NiCu electrode experienced immersing in 0.5 M $CuCl_2$ for 1 h and 3 CV treatment number (HSN-3). A simple Randle's cell is shown in the inset. (b) Tafel plots of Ni foam, D NiCu electrode obtained by immersing Ni foam in 0.5 M $CuCl_2$ for 1 h and HSN-3.

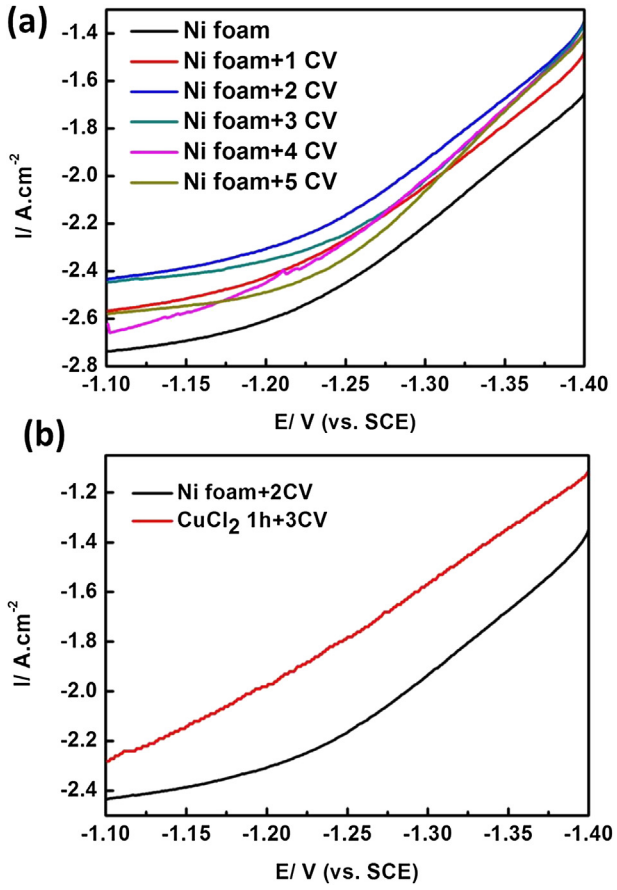

Fig. 12. (a) Polarization curves of Ni foam which directly experienced different CV number. (b) Polarization curves of Ni foam which directly experienced 2 CV and hierarchically structured NiCu electrode experienced immersing in 0.5 M $CuCl_2$ for 1 h and 3 CV treatment number (HSN-3).

same electrode. However, some difference exists for different electrodes. This may be attributed to the differing metal dissolutions in different systems.

Fig. 11b displays the tafel plots of Ni foam, 3D NiCu electrode obtained by immersing Ni foam in 0.5 M $CuCl_2$ for 1 h and HSN-3. The obtained tafel slope and HER current were given in Table 3. We can know from the data that these three electrode exhibit similar HER mechanism. The HER current of Ni foam is the lowest, and that of HSN-3 is the highest. These result is coincided with our previous polarization and EIS curves. The variances which originated form the selection of tafel region were also given in Table 3.

The comparison of Ni foam, 3D NiCu precursor and HSN electrodes further confirmed the feasibility of our method to prepare HSN electrodes with high HER activity.

Fig. 12a shows the polarization curves of Ni foam which directly experienced different CV treatment number. It can be seen that Ni foam experienced 2 CV was the most active electrode. Fig. 12b displays the polarization curves of Ni foam which directly experienced 2 CV and HSN-3. It is evident that HSN-3 has much higher HER activity. This comparison prove that directly CV treatment can not get electrode which has high HER activity.

4. Conclusions

3D NiCu precursors were prepared by dipping Ni foam in copper ion solutions followed by GRR between Ni and Cu^{2+}. Three different dipping solutions with the same molar concentration were employed. The results confirmed that $CuCl_2$ is the best solution with an optimal dipping time of 1 h. This may be attributed to the adsorption of chloride ion on the copper surface, formation of $CuCl_n^{1-n}$ complex and hydrolysis of $CuCl_n^{1-n}$, which promote GRR between Ni and Cu^{2+}. After an activation process, a CV treatment was performed. A HSN electrode can be fabricated by the combination of GRR and CV treatment. The surface area was further improved, heightening the HER activity. The optimal number of CV cycles is 3.

Acknowledgments

This study was supported by the National Natural Science Foundation of China (grant nos. 51271148 and 50971100), the Research Fund of State Key Laboratory of Solidification Processing in China (grant no. 30-TP-2009), and the Aeronautic Science Foundation Program of China (grant no. 2012ZF53073), and the Doctoral Fund of Ministry of Education of China (grant no. 20136102110013).

References

[1] R. Subbaraman, D. Tripkovic, N.M. Markovic, Science 334 (2011) 1256.
[2] Y.G. Li, H.L. Wang, L.M. Xie, J. Am. Chem. Soc. 133 (19) (2011) 7296–7299.
[3] A.B. Papandrew, T.A. Zawodzinski Jr., J. Power Source 245 (2014) 171–174.
[4] M.Y. Wang, Z. Wang, X.Z. Gong, Renew. Sustain. Energy Rev. 29 (2014) 573–588.

[5] J.R. McKone, B.F. Sadtler, C.A. Werlang, ACS Catal. 3 (2013) 166–169.
[6] Z.W. Yin, F.Y. Chen, Surf. Coat. Technol. 228 (2013) 34–40.
[7] B.M. Jovic, U.C. Lacnjevac, N.V. Krstajic, Electrochim. Acta 114 (2013) 813–818.
[8] W.F. Chen, K. Sasaki, C. Ma, Angew. Chem. Int. Ed. 51 (2012) 6131–6135.
[9] R. Ojani, J.B. Raoof, E. HSNheminejad, Int. J. Hydrogen Energy 38 (2013) 92–99.
[10] Y.G. Sun, Y.N. Xia, Nano Lett. 3 (11) (2003) 1569–1572.
[11] V. Bansal, A. O'Mullane, S.K. Bhargava, Electrochem. Commun. 11 (2009) 1639–1642.
[12] D.H. Wan, X.H. Xia, Y.C. Wang, Small (2013), http://dx.doi.org/10.1002/smll.201203233.
[13] L. Chen, L. Kuai, X. Yu, Chem. Eur. J. 19 (35) (2013) 11753–11758.
[14] H. Xing, J.J. Long, F.Z. Hui, J. Electrochem. Soc. 160 (9) (2013) A1425–A1429.
[15] Z.W. Yin, F.Y. Chen, Electrochim. Acta 117 (2014) 84–91.
[16] R. Solmaz, A. Doner, G. Kardas, Electrochem. Commun. 10 (2008) 1909–1911.
[17] R. Solmaz, A. Dner, G. Kardas, Int. J. Hydrogen Energy 34 (5) (2009) 2089–2094.
[18] C.S. Wang, W. Li, X.H. Lu, Int. J. Hydrogen Energy 37 (2012) 18688–18693.
[19] M.J. Giz, M.C. Marengo, E.A. Ticianelli, Ecletica Quimica 28 (2) (2003) 21–28.
[20] V. Bansal, H. Jani, J.D. Plessis, Adv. Mater. 20 (2008) 717–723.
[21] J.M. Droog, C. Alderliesten, P. Alderliesten, J. Electroanal. Chem. Interfacial Electrochem. 111 (1) (1980) 61–70.
[22] S.L. Marchiano, C.I. Elsner, A.J. Arvia, J. Appl. Electrochem. 10 (1980) 365–377.
[23] A. Radi, D. PradHSN, Y.K. Sohn, ACS Nano 4 (3) (2010) 1553–1560.
[24] K. Ngamlerdpokin, N. Tantavichet, Int. J. Hydrogen Energy 39 (6) (2013) 2505–2515.
[25] J. Creus, H. Mazille, H. Idrissi, Surf. Coat. Technol. 130 (2000) 224.